APPLIED AND ENVIRONMENTAL MICROBIOLOGY, Oct. 2005, p. 6086–6095 Vol. 71, No. 10
0099-2240/05/$08.00+0 doi:10.1128/AEM.71.10.6086–6095.2005

Bioaerosol Mass Spectrometry for Rapid Detection of Individual Airborne *Mycobacterium tuberculosis* H37Ra Particles

Herbert J. Tobias,[1] Millie P. Schafer,[2] Maurice Pitesky,[1] David P. Fergenson,[1] Joanne Horn,[1] Matthias Frank,[1] and Eric E. Gard[1]*

Lawrence Livermore National Laboratory, Livermore, California,[1] and National Institute for Occupational Safety and Health, Cincinnati, Ohio[2]

Received 2 March 2005/Accepted 22 April 2005

Single-particle laser desorption/ionization time-of-flight mass spectrometry, in the form of bioaerosol mass spectrometry (BAMS), was evaluated as a rapid detector for individual airborne, micron-sized, *Mycobacterium tuberculosis* H37Ra particles, comprised of a single cell or a small number of clumped cells. The BAMS mass spectral signatures for aerosolized *M. tuberculosis* H37Ra particles were found to be distinct from *M. smegmatis*, *Bacillus atrophaeus*, and *B. cereus* particles, using a distinct biomarker. This is the first time a potentially unique biomarker was measured in *M. tuberculosis* H37Ra on a single-cell level. In addition, *M. tuberculosis* H37Ra and *M. smegmatis* were aerosolized into a bioaerosol chamber and were sampled and analyzed using BAMS, an aerodynamic particle sizer, a viable Anderson six-stage sampler, and filter cassette samplers that permitted direct counts of cells. In a background-free environment, BAMS was able to sample and detect *M. tuberculosis* H37Ra at airborne concentrations of >1 *M. tuberculosis* H37Ra-containing particles/liter of air in 20 min as determined by direct counts of filter cassette-sampled particles, and concentrations of >40 *M. tuberculosis* H37Ra CFU/liter of air in 1 min as determined by using viable Andersen six-stage samplers. This is a first step toward the development of a rapid, stand-alone airborne *M. tuberculosis* particle detector for the direct detection of *M. tuberculosis* bioaerosols generated by an infectious patient. Additional instrumental development is currently under way to make BAMS useful in realistic environmental and respiratory particle backgrounds expected in tuberculosis diagnostic scenarios.

Tuberculosis, the disease caused by *Mycobacterium tuberculosis*, is currently a worldwide epidemic. Over 8 million cases were reported and nearly 2 million people died of tuberculosis in 2000; it is second only to human immunodeficiency virus/AIDS (5, 10). Airborne *M. tuberculosis* particles ranging in size from 1 to 5 μm are transmitted from the respiratory effluent of infected individuals and are prevalent in areas such as hospitals, prisons, homeless shelters, drug treatment centers, and other institutional settings (14, 46). Real-time detection of airborne environmental *M. tuberculosis* particles could help identify infected individuals and improve response and management to mitigate the spread of the disease.

Many tests to diagnose tuberculosis in patients are currently used; however, the actual techniques used depend on the setting and vary in their sensitivity, specificity, speed, and cost (12). Collection of samples for traditional culture methods on solid media are considered the standard and can range from simple and inexpensive (sputum swabs) to difficult and painful (gastric lavage). Unfortunately, *M. tuberculosis* is a slow-growing *Mycobacterium* for which growth-dependent tests are time-consuming and can take up to several weeks for reliable results. The time requirement of such assays dangerously lags the pace of life in modern urban societies. In addition, naturally occurring aerosolized environmental mycobacteria may not be viable, and those that are viable may not be culturable (22, 42, 47). On the other hand, the Ziehl-Neelsen diagnostic method is one of the simplest and most rapid of techniques and uses staining and smear microscopy to detect acid-fast bacilli. However, it is insensitive, requiring 10^4 bacilli/ml of liquid, and is characterized by low specificity since it cannot differentiate *M. tuberculosis* from other mycobacteria. Serological techniques such as antibody-based enzyme immunoassays and molecular amplification methods such as PCR are much more specific, are highly sensitive, and can be performed more rapidly but still take hours to perform (17, 45).

Apart from genetic molecular information, some important chemical components have been used to discriminate between *M. tuberculosis* and other mycobacteria and/or microorganisms. Identification of tuberculostearic acid by gas chromatography-mass spectrometry has been shown to be a good marker for diagnosis of *M. tuberculosis*; however, this lipid can also be found in *M. bovis*, *M kansasii*, and *M. africanum* (24). The detection of the glycolipid, lipoarabinomannan, which composes up to ~15% of the dry weight of the cell, has also been demonstrated for diagnostic purposes but again is not unique to *M. tuberculosis* (15). More generally, determination of the specific cell protein composition has been popular and shown to be useful for some discrimination of various species of microbes using matrix-assisted laser–desorption ionization mass spectrometry of intact microorganisms (3, 7, 23). More specifically, nuclear magnetic resonance spectroscopy (48), mass spectrometry (20), and high-performance liquid chromatography (4) have been used to obtain profiles of mycolic acids, which make up 40 to 60% of the dry weight of mycobacteria (2) and have been shown to be fairly specific to many species of mycobacteria.

* Corresponding author. Mailing address: L-452 Lawrence Livermore National Laboratory, 7000 East Ave, Livermore, CA 94550. Phone: (925) 422-0038. Fax: (925) 422-3570. E-mail: gard2@llnl.gov.

Some of these methods can be used to help detect and identify airborne *M. tuberculosis* if coupled to appropriate air collection devices utilizing suitable substrates. Aerosolized *M. bovis* BCG and the avirulent *M. tuberculosis* H37Ra, surrogates for pathogenic *M. tuberculosis*, have previously been successfully sampled in a laboratory bioaerosol chamber (CDC-NIOSH, Cincinnati, OH) (35–37). These studies used viable Andersen six-stage samplers and eight-stage micro-orifice uniform deposit impactors containing Teflon filters for particle size fractionation. Disposable filter cassette samplers were also used as simple, sensitive filter collection samplers for airborne mycobacteria. The mycobacteria were readily detected by using PCR. Another study investigated aerosols of artificial saliva containing *M. avium*, *M. intracellulare*, and *M. tuberculosis* that were generated in a class III safety cabinet and sampled and analyzed by using viable Andersen six-stage samplers and viable all-glass impingers (21). Some of these techniques were subsequently applied, in the field, to the detection and characterization of mycobacteria associated with whirlpools at a large public facility (37). Also for the first time, the size range and concentrations of infectious tuberculosis aerosols were directly measured from culturable cough-generated aerosols of *M. tuberculosis* from infected human test subjects by using Andersen six-stage samplers with culturing (6). In that study, concentrations of airborne *M. tuberculosis* particles were measured at approximately 1 to 2 CFU/liter of air when sufficiently infected individuals repeatedly coughed into a small chamber for 5 min. All of these studies used methods that required only a few minutes for sampling the aerosols. Subsequent offline analysis for detection and characterization took approximately a few hours using the nonculturing techniques and up to a few weeks using the culturing techniques.

A rapid, reagentless on-line analytical technique to sample and detect bioaerosols, at the individual particle-level of resolution, called bioaerosol mass spectrometry (BAMS), is being developed at Lawrence Livermore National Laboratory for national security and public health applications that require detection of airborne bio-agents such as vegetative bacteria, bacterial spores, viruses, and biological toxins (8, 34, 41). Although the size and cost of BAMS is currently greater than some other techniques, it will be useful where real-time, unmanned, continuous operation is required, and development of a smaller and less-expensive version is under way. The BAMS technique is based on single-particle aerosol mass spectrometry (11, 18, 19, 25, 29, 30, 43, 44), which has previously been applied to the analysis of a range of biological particles (13, 16, 31, 38, 39). This is the first time it has been used to analyze *M. tuberculosis*. In BAMS, many individual airborne particles are sampled per second directly from the air and accelerated to size-dependent speeds in a vacuum system, where the individual particles are then individually sized by the time delay measured between two laser scattering events. The molecules in the particles are then desorbed and ionized using high-power 266-nm laser light, and the fragments are chemically analyzed by using dual polarity time-of-flight mass spectrometry (TOF-MS). BAMS has already been shown to be a promising technique for the detection of *Bacillus* spores of interest to biodefense applications, and the differentiation of two *Bacillus* spore species was demonstrated (8). BAMS is currently being developed further as an analytical method for the rapid, noninvasive diagnostics of infectious disease in respiratory effluent. Such a method would permit a more rapid response to public health concerns associated with diseases, such as tuberculosis and influenza.

Here we present the first results from an evaluation of BAMS for the rapid real-time detection of airborne mycobacteria using aerosolized forms of the avirulent variant *M. tuberculosis* H37Ra and *M. smegmatis* in a bioaerosol chamber. The signatures of these organisms are also compared to other gram-positive vegetative bacteria, *B. atrophaeus* and *B. cereus*. For the first time, the accuracy and sensitivity of BAMS is quantitatively established using an aerodynamic particle sizer (APS), viable Andersen six-stage samplers, and disposable filter cassette samplers, which permitted direct counts of the collected airborne mycobacteria cells.

MATERIALS AND METHODS

Culture preparations. Stocks of *M. tuberculosis* H37Ra (ATCC 25177) and *M. smegmatis* (ATCC 19420) were cultured on Lowenstein-Jensen Gruft slants (Difco Laboratories, Detroit, MI) at 37°C in 7.5% CO_2 and then stored at 4°C. Broth cultures of mycobacteria were grown in Bacto Dubos broth (5% glycerol, 0.25% Tween 80) at 35 to 37°C and vortexed daily to minimize clumping. The initial number of rod-shaped mycobacteria particles/ml in early or mid-log-phase liquid culture was determined by using a Petroff Hausser Counting Chamber (Hausser Scientific Partnership, Horsham, PA). Approximately 70 to 90% of the cells in the culture appeared as single or double rods. The remaining percentage of cells, in general, contained three to five cells. No large clumps, containing 10 or more mycobacteria, were present. The cells were subjected to centrifugation at 1,500 × *g* for 5 min, followed by resuspension in sterile water. This washing step was conducted twice.

B. atrophaeus (ATCC 9372) and *B. cereus* (ATCC 14579) were prepared as vegetative cells (i.e., nonspores). Stocks of these organisms were cultured in Nutrient Broth (Difco Laboratories, Detroit, MI) from a single colony isolated from a streak plate until turbid (after approximately 12 h). The cells were then subcultured at a 1:200 dilution and grown overnight in Nutrient Broth at 37°C in a shaker incubator. Finally, the cells were then centrifuged at 8,000 × *g* for 10 min and washed with sterile distilled water. This washing step was conducted three times.

APS. An APS (model 3321; TSI, Inc., St. Paul, MN) was used to independently measure particle sizes and particle concentrations in the aerosol sampled in experiments characterizing the various stages of the BAMS system and in the aerosol sampled in the bioaerosol chamber experiments (both described below). The APS is a widely used technique that measures the concentration and aerodynamic diameter of individual particles (0.5 to 20 μm in diameter) by sampling and accelerating them to size-dependent speeds measured by two continuous wave lasers. For these experiments, the APS was run in the summed mode. Particles measured in bin 1 (<0.523 μm in diameter) were not used. It has been shown that the APS TSI 3221 particle counting efficiencies are roughly constant at ~50% in the particle size range of this study compared to impactor sampling (32); therefore, measured APS concentrations were corrected by a factor of 2.

BAMS: overview. An aerosol time-of-flight mass spectrometer (model 3800; TSI) based on a transportable design (11) was used with modifications, as previously described in detail (8, 34, 41) and referred to here as BAMS (Fig. 1A). Briefly, airborne particles and air were sampled into a two-stage virtual impactor (VI, MVA-400; MesoSystems, Kennewick, WA) at 400 liters/min. This was used to concentrate particles with diameters greater than 2 μm by a factor of 120 into the airflow that was sampled into the BAMS vacuum system. The VI stage was designed for an output minor flow of 3 liters/min; therefore, since only 0.9 liters/min of the minor flow was sampled into the BAMS vacuum system, the remaining flow was made up by a split off to a small vacuum pump. This made the effective sampling rate of BAMS approximately 120 liters/min. Within the BAMS apparatus, the preconcentrated aerosol was sampled into a differentially pumped vacuum system through a converging nozzle. Particles were accelerated into a high-vacuum region according to their aerodynamic diameters and individually sized by the time delay measured between two scattering lasers when a single particle passes through them. The measured particle speed was used to predict its arrival in the center of the ion source of a dual-polarity reflectron time-of-flight mass spectrometer. In the ion source, molecules from the particle were desorbed and ionized by using a frequency-quadrupled, Q-switched Nd:

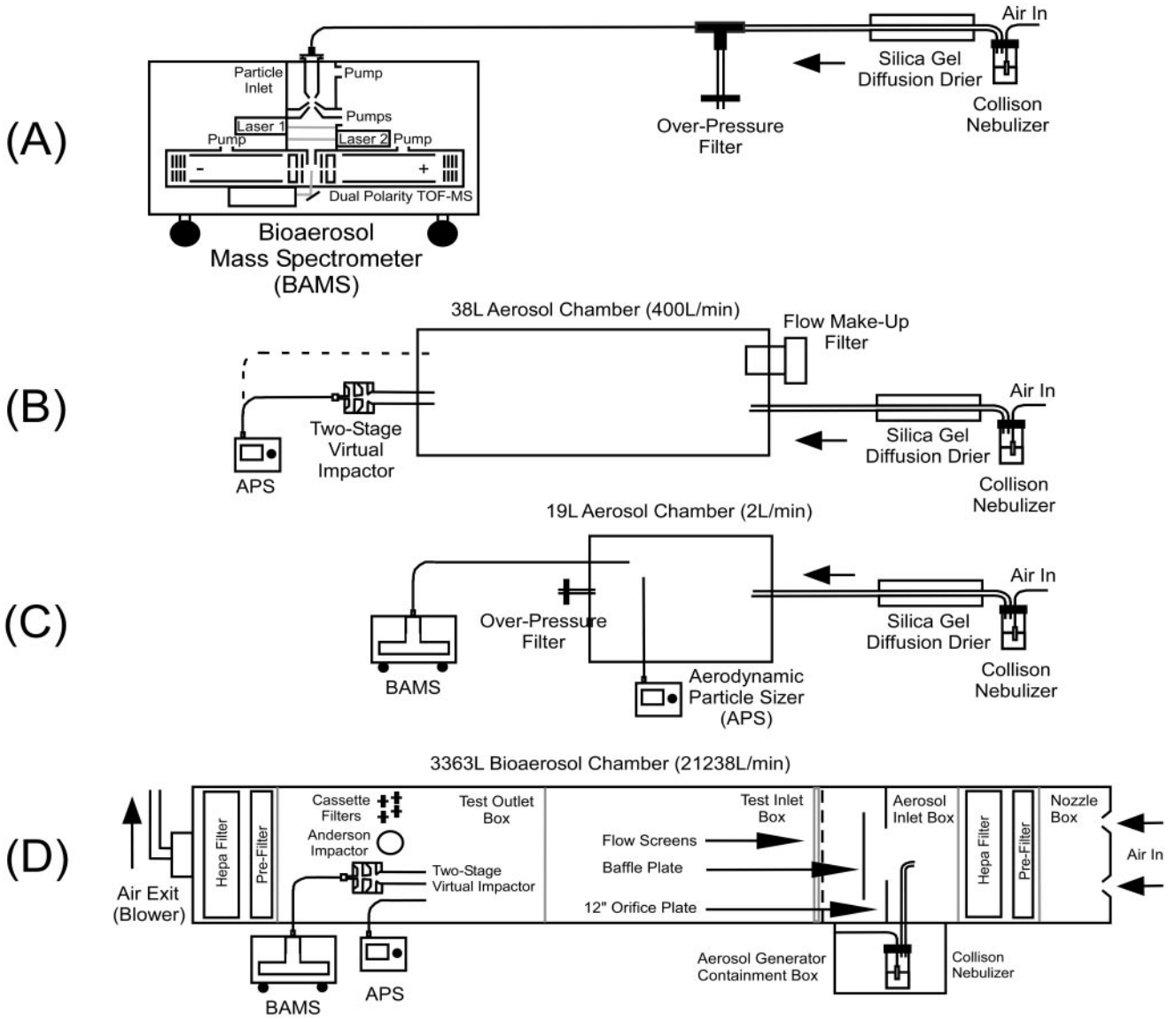

FIG. 1. Schematic of aerosol generation, sampling, and detection experimental setups for BAMS mass spectral signature development using BAMS without its virtual impactor (VI) stage (A), BAMS' virtual impactor (VI) stage efficiency measurements (B), BAMS particle sampling and tracking efficiency measurements using BAMS without its VI stage (C), and the CDC-NIOSH bioaerosol chamber experiments (D).

YAG laser. The laser power used was ~660 μJ per pulse, and the laser beam diameter in the center of the ion source was ~400 μm in diameter, resulting in a laser fluence of ~0.5 J/cm^2 (41). Both positive and negative ions were simultaneously extracted in opposite directions and analyzed by TOF-MS for single particle chemical analysis.

BAMS: mass spectral signature development. BAMS mass spectral signatures for *M. tuberculosis H37R*, *M. smegmatis*, *B. atrophaeus*, and *B. cereus* were developed using the BAMS without the VI stage in-line. An aerosol of a liquid suspension of mycobacteria cells of approximately 10^6 cell/ml was generated by using a single-jet Collison nebulizer (TSI) directed through a diffusion drier filled with silica gel and then sampled directly into the BAMS, as depicted in Fig. 1A.

BAMS: sampling efficiency measurements. Particle sampling and detection efficiencies of the various stages of BAMS were determined to enable the calculation of absolute particle concentrations from BAMS measurements. Aerosol preconcentration efficiency by the VI stage was characterized by continuous aerosolization of monodisperse polystyrene latex microspheres (PSLs; Duke Scientific) into a small aerosol chamber (38 liters) using a collision nebulizer, as shown in Fig. 1B. A total chamber flow of ~400 liters/min was set by the VI, which comprised of ~3 liters of aerosolized PSLs/min and ~397 liters of filtered room air/min. An APS was used to measure the aerosol concentrations. Here, only the internal nozzle of the APS was used to sample directly from the chamber at 1 liter/min, and the 4 liters of filtered sheath air for the APS/min was sampled from the room air. In order to calculate the overall preconcentration of particles with a specific aerodynamic diameter, aerosol concentrations measured in 1 liter/min of a total of 3 liters/min VI exit minor flow (Fig. 1B, solid line) was compared to the aerosol concentrations measured before entering the VI (dashed line).

The BAMS particle sampling and tracking efficiency for the stages after the VI was also characterized. Monodisperse PSLs of 0.5 to 5.0 μm in diameter were aerosolized into a small aerosol chamber (19 liters) using a collision nebulizer, as shown in Fig. 1C. BAMS and an APS simultaneously sampled from the chamber aerosol. The number of particles successfully tracked and sized by BAMS was compared to the particle concentration measured by the APS.

The ability to produce mass spectra from individual *Mycobacterium* particles was determined by measuring the fractional hit rate of the particles. The fractional hit rate was defined as the fraction of particles whose molecules were desorbed, ionized, and produced sufficient ions for a mass spectrum out of all of

the particles that were successfully tracked and sized in BAMS. This rate is dependent on the particle type and size.

Particle transport efficiencies were also experimentally measured in the sample tubing (3/8-in.-inner-diameter copper; Swagelok; Oakland Valve, Oakland, CA) that led from the bioaerosol chamber to the APS and that led from the virtual impactor to the converging nozzle of the BAMS system. The particle losses for both systems were determined to be <5%.

Bioaerosol experiments: general protocol. A typical bioaerosol chamber experiment was conducted as follows. Details are provided in the sections provided below. A *Mycobacterium* strain was cultured and washed. The concentration of mycobacteria in the suspension was determined. The suspension was diluted in sterile water to a desired concentration and transferred to a Collison nebulizer. Aerosolization began when clean air flow through the Collison nebulizer was started and was continued for 20 min. Sampling by all of the techniques was started when aerosolization began. The viable Andersen six-stage sampler was run for only the first 60 s of aerosolization. The BAMS, APS, and filter cassette samplers were run for the full 20 min of aerosolization.

Bioaerosol experiments: bioaerosol chamber. The overall experimental setup at NIOSH (Cincinnati, OH) is depicted in Fig. 1D. As previously described (35–37), the NIOSH bioaerosol chamber (Torrington Research Company, Torrington, CT) was constructed of stainless steel and measured 30 in. by 30 in. by 19 feet (3,363 liters). The biochamber contained baffles downstream of the aerosol inlet in order to generate a uniform bioaerosol concentration within the chamber. The supply and exhaust air were purified by passing the air through prefilters and high-efficiency particulate air filters. The velocity throughout the cross-sectional area of the sampler location was uniform and determined to be approximately 100 feet/min (21,238 liters/min).

Bioaerosol experiments: microbial aerosol generation. For both *M. tuberculosis* H37Ra and *M. smegmatis*, aliquots of the washed cells were diluted to three final concentrations of $\sim 1 \times 10^7$, $\sim 5 \times 10^7$, and $\sim 1 \times 10^8$ cells/ml. Approximately 50 to 100 ml of microbial suspension was placed in a six-jet modified MRE-type Collison nebulizer (BGI, Inc., Waltham, MA). Filtered compressed air (138 kPa) was used to generate the bioaerosols for 20 min. Negative controls for all samplers were obtained by operating the chamber under conditions similar to the microbial aerosolization experiments, omitting the microbial suspension.

Bioaerosol experiments: Andersen six-stage sampling and analysis. A viable Andersen six-stage particle sizing sampler (Graseby Andersen Division, Smyrna, GA) positioned directly inside the bioaerosol chamber (Fig. 1D) was used to quantify the number of culturable airborne mycobacteria and for the determination of the aerodynamic diameter 50% cut point range of the aerosolized mycobacteria. The device sampled at a flow rate of 28.3 liters/min and was loaded with Bacto Dubos oleic agar plates (Difco). Sampling was conducted for 1 min during the initial phase of the mycobacteria bioaerosol generation period. The sampling time was limited to 1 min because longer sampling times at the cell aerosol concentrations generated would overload the sampler, preventing the ability to quantify. After sample collection, the agar plates were removed and incubated at 37°C in 7.5% CO_2 for 2 to 3 weeks. The plates were examined daily for the presence of mycobacterium colonies. Visible colonies were manually counted on a model C-110W colony counter (New Brunswick Scientific Co., Edison, NJ). A positive hole conversion table was applied to correct for statistical effects (1).

Bioaerosol experiments: filter cassette sampling and analysis. A three-piece filter cassette sampler (Gelman Sciences, Ann Arbor, MI) positioned directly inside the bioaerosol chamber (Fig. 1D) was used for direct cell counts of airborne mycobacteria in the bioaerosol chamber. The cassettes contained 37-mm PTFE filters (Costar no. 130810) with a 1.0-μm pore size. The airflow rate through the filter cassette sampler was 3.7 liters/min, and sampling was conducted for 20 min. After sample collection, the filters were treated with SYBR Green I nucleic acid gel stain (FMC BioProducts), and the cells were directly counted using an Olympus fluorescence microscope (B&B Microscopes, Ltd., Warrendale, PA). SYBR Green I is a highly sensitive fluorescent stain that binds to nucleic acids in the bacterial cells.

Bioaerosol experiments: BAMS sampling. BAMS measurements of bioaerosol chamber samples were sampled directly, with the VI stage situated directly inside the chamber and positioned parallel to the aerosol flow path as depicted in Fig. 1D. The system sampled at a flow rate of 400 liters/min for 20 min. The first minute of BAMS sampling was used for comparison to the Andersen six-stage sampler and APS measurements. The full 20 min of BAMS sampling was used for comparison to the filter cassette sampler measurements.

Bioaerosol experiments: APS sampling. APS measurements of bioaerosol chamber samples were made by using a 3/8 in.-inner-diameter copper sampling tube (Swagelok), which was situated directly inside the chamber and positioned parallel to the aerosol flow path as depicted in Fig. 1D. The APS sampled at a flow rate of 5 liters/min for 20 min. The first minute of APS sampling was compared to the BAMS results.

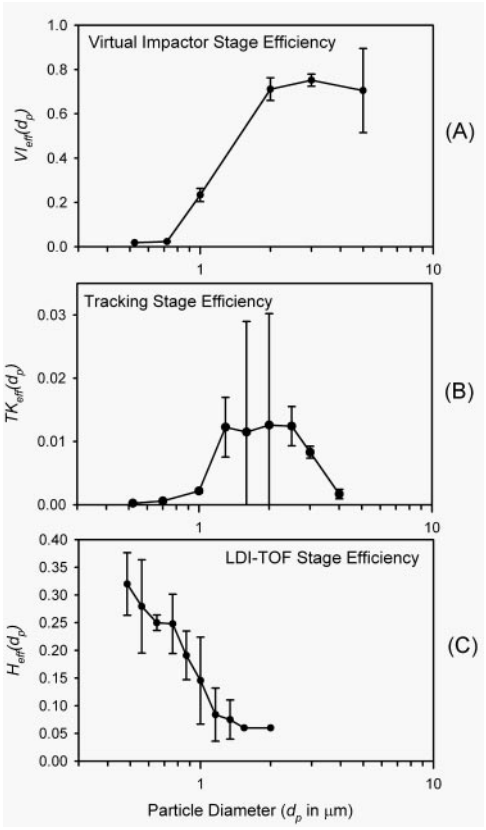

FIG. 2. Experimentally measured particle preconcentration, sampling, and detection efficiencies for the various stages of the BAMS. (A) Fractional efficiency with which particles are concentrated in the virtual impactor (VI) stage exit minor flow as a function of particle diameter [$VI_{\text{eff}}(d_p)$]. This is based on a theoretical concentration factor of 120. (B) Fraction of particles successfully tracked and sized out of all particles that are sampled by the BAMS after the VI stage as a function of particle diameter [$TK_{\text{eff}}(d_p)$]. (C) Fractional hit rate, defined as the fraction of particles whose molecules are desorbed, ionized, and produced a mass spectrum out of all particles successfully tracked and sized by the BAMS as a function of particle diameter [$H_{\text{eff}}(d_p)$]. This was measured with 1,000 *M. tuberculosis* H37Ra- and 1,000 *M. smegmatis*-containing particles.

Bioaerosol experiments: calculation of aerosol concentrations measured by BAMS. Particle sampling and detection efficiencies at numerous stages of BAMS were quantitatively determined as described above. The preconcentration of aerosol particles by the VI stage of BAMS was characterized. The VI stage was designed to concentrate particles with diameters of greater than 2 μm in air by a factor of 120. Figure 2A shows the fractional efficiency with which the VI stage concentrated particles with diameters in the range of 0.5 to 5.0 μm. In addition, Fig. 2B shows the fractional efficiency by which particles are successfully tracked and sized in BAMS, as a function of particle diameter. Furthermore, Fig. 2C shows the fractional hit rate measured for a combination of 1,000 *M. tuberculosis* H37Ra and 1,000 *M. smegmatis* particles, as a function of particle diameter in the range of 0.5 to 2.0 μm. The fractional hit rate was defined as the fraction of particles whose molecules were desorbed, ionized, and produced sufficient ions for a mass spectrum out of all of the particles that were successfully tracked and sized. Using these efficiencies, the aerosol concentration was calculated as measured by BAMS in units of particles/liter of air by using the following equations.

The concentration of total particles, regardless of their identity, was calculated as follows:

TABLE 1. Overview of the capabilities of the techniques used in this study

Technique	Feature[a]			
	Particle counter	Particle sizer	Cell counter	Cell identifier
APS (real-time)	X	X		
Direct counts of filter cassette sampler collected cells			X	
Viable Andersen six-stage sampler		X	X	X
BAMS (real-time)	X	X	X	X

[a] X, feature present.

$$C_{\text{total}} = \sum_{d_p} C = \sum_{d_p} \frac{N_{\text{track}}(\text{d}_\text{p})}{\text{T} \times 120 \times \text{TK}_{\text{eff}}(d_p) \times VI_{\text{eff}}(d_p)} \quad (1)$$

where d_p is the diameter of the particle, N_{track} is the number of particles tracked and sized by the scattering lasers during the measurement, T is the total time of the measurement in minutes, 120 is the effective sampling rate of the BAMS system in liters/minute, TK_{eff} is the fractional efficiency with which particles are tracked and sized by BAMS (these values are presented in Fig. 2B), and VI_{eff} is the fractional efficiency with which the virtual impactor (VI) concentrates the sampled aerosol. These values are presented in Fig. 2A and are based on a theoretical concentration factor of 120.

The concentration of particles classified as "vegetative cell" or *M. tuberculosis* H37Ra-containing particles was calculated as follows:

$$C_{\text{classified}} = \sum_{d_p} C(d_p) \times \frac{N_{\text{classified}}(d_p)}{N_{\text{track}}(d_p) \times H_{\text{eff}}(d_p) \times CL_{\text{eff}}} \quad (2)$$

where $N_{\text{classified}}(d_p)$ is the number of particles classified as vegetative cell or *M. tuberculosis* H37Ra-containing particles during the measurement, and H_{eff} is the fractional efficiency with which mycobacteria particles were hit (of all particles that were successfully tracked and sized). These values are presented in Fig. 2C. Also, CL_{eff} is the fractional efficiency with which particles were classified as vegetative cell (0.93) or *M. tuberculosis* H37Ra ($0.93 \times 0.66 = 0.614$)-containing particles out of all standard vegetative-cell- or *M. tuberculosis* H37Ra-containing particles hit, respectively. The source of these values is discussed below.

Using these equations, the concentration of particles present in the bioaerosol chamber samples was calculated from the number of particles measured by BAMS.

Technique matrix. An overview of the capabilities of the techniques used here is presented in Table 1. For instance, the APS was used to measure particle concentrations in air and their relative sizes (0.5 to 20 μm) but could not identify them. The SYBR green I fluorescent cell stain counts of filter cassette-sampled particles were used to directly count the viable and nonviable cells in the sampled air. The viable Andersen six-stage sampler was used to quantify the concentration of viable cells that are culturable and measure their aerodynamic size. BAMS was used to quantify total airborne particles and their sizes and identify particles containing viable and nonviable cells. Among these techniques, only the APS and BAMS performed real-time measurements on individual airborne particles.

RESULTS AND DISCUSSION

BAMS single particle mass spectra signature development. During mass spectral signature development, BAMS provided individual dual-polarity mass spectra from single *M. tuberculosis* H37Ra-, *M. smegmatis*-, *B. atrophaeus*-, and *B. cereus*-containing particles comprised of a single cell or a small number of clumped cells. Figure 3 shows the average of ~1,000 single-particle BAMS mass spectra from ~1,000 single airborne *M. tuberculosis* H37Ra, *M. smegmatis*, *B. atrophaeus*, and *B. cereus* particles. Averages are shown for clarity since laser shot-to-shot variations of individual mass spectral signatures were observed. An example of these fluctuations is shown by a series of individual particle mass spectra of *M. tuberculosis* H37Ra containing particles in Fig. 4. These variations may be due to fluctuations in absorbed laser energies and biological composition, as previously described for BAMS analysis of *Bacillus* spores (41). The overall single particle BAMS mass spectra of *M tuberculosis* H37Ra, *M. smegmatis*, *B. atrophaeus*, and *B. cereus* looked similar to each other (Fig. 3) A novel pattern recognition algorithm (8), which is similar to an ART-2a clustering algorithm previously described (33, 40), was used in the analysis of individual BAMS mass spectra and classified single particle types in real time. Used on its own, this data analysis scheme could not efficiently differentiate between these vegetative bacterial cells. Nevertheless, this scheme could be used to efficiently differentiate these organisms from other particle types, such as bacterial spores and environmental particles, and classify them as "vegetative cells." Once a particle was classified as a vegetative cell using the pattern recognition algorithm, a rule-based method using the presence of unique marker *m*/*z* peaks over a certain signal threshold was used to further classify the vegetative bacterial cell; this method was also previously described in detail (8). With the BAMS mass spectral signatures developed in the present study, it was found that BAMS with pattern recognition analysis classified *M. tuberculosis* H37Ra and *M. smegmatis* containing particles as vegetative cells at a rate of ~93%. The remaining 7% of the spectra in the data set were either not able to be classified by the algorithm or were not spectra of actual vegetative cells and were classified as unknown. Using a unique marker peak at *m*/*z* −421 in the BAMS mass spectra of individual *M. tuberculosis* H37Ra-containing particles (Fig. 3), BAMS with rule-based differentiation further classified *M. tuberculosis* H37Ra at a rate of ~66% at an absolute specificity compared to *M. smegmatis*. This means that when 1,000 individual spectra of *M. tuberculosis* H37Ra were compared to 1,000 individual spectra of *M. smegmatis*, the signal level of *m*/*z* −421 was above a threshold that positively identified 660 individual spectra as *M. tuberculosis* H37Ra, and none of the *M. smegmatis* spectra were misidentified as *M. tuberculosis* H37Ra. In addition, when similarly compared to the other gram-positive vegetative bacteria, *B. atrophaeus* and *B. cereus*, *M. tuberculosis* H37Ra was positively classified at rates of ~73 and ~69%, respectively, indicating the *m*/*z* −421 peak is potentially unique to *M. tuberculosis* H37Ra. This is the first time a potentially unique biomarker was measured in *M. tuberculosis* H37Ra at the single-cell and single-particle level in real time.

In addition to mycolic acids (2), potential sources of biomarkers may include bacterial cell wall components such as lipopolysaccharides and muramic acid (9). A trehalose-2-sulfate metabolite, which functions as a required precursor to the biosynthesis of the potential virulence factor sulfolipid, 2,3,6,6′-tetraacyl-α,α′-D-trehalose-2′-sulfate known as sulfolipid 1 (SL-1) (26, 28, 49), has previously been positively identified as a component of the virulent *M. tuberculosis* H37Rv and *M. smegmatis* cells (27). This disaccharide was detected in its deprotonated form at *m*/*z* −421 in negative ion mass spectra utilizing Fourier transform-ion cyclotron resonance mass spectrometry of crude bulk cell extracts, but its relative abundance was not determined (27). We suggest that the *m*/*z* −421 peak associated with *M. tuberculosis* H37Ra in the BAMS mass spectra is tentatively due to the deprotonated disaccharide, trehalose-2-sulfate ion (Fig. 4A). Two fragment ions, *m*/*z* 241

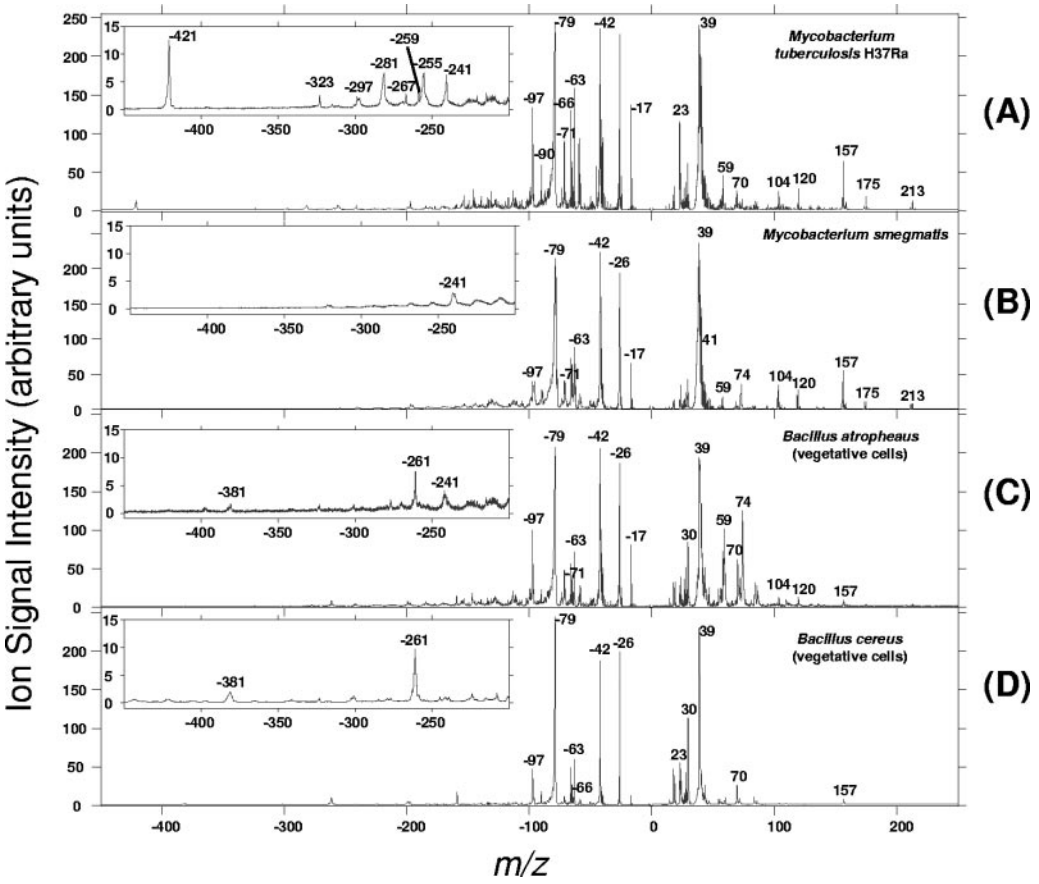

FIG. 3. Average of ~1,000 single particle BAMS mass spectra of airborne *M. tuberculosis* H37Ra (A)-, *M. smegmatis* (B)-, *B. atrophaeus* (C)-, and *B. cereus* (D)-containing particles. Many of the individual spectra of *M. tuberculosis* H37Ra-containing particles (~66%) can be differentiated from the three other organisms based on the presence of a m/z −421 peak.

and 259, representing the fragmentation of the disaccharide at either side of the oxygen link, were also present. We believe the absence of m/z −421 in the BAMS mass spectrum of *M. smegmatis* could be due to a significantly lower abundance of trehalose-2-sulfate, one that is below the intracellular detection limit of BAMS, since *M. smegmatis* is known not to produce SL-1. In future work, synthesis of a standard of trehalose-2-sulfate will be pursued in order to help authenticate the identity of this m/z −421 marker peak and further explore the intracellular concentrations and the robustness of this biomarker and other potential biomarkers.

Quantitative analysis of bioaerosol chamber samples. Figure 5A and B show an example size distribution of the raw number of particles measured and the resulting calculated concentrations for each particle size, regardless of their identity. These were measurements made by APS and BAMS, respectively, in the bioaerosol chamber sample generated in the first 60 s of aerosolization of $\sim 10^8$ *M. smegmatis* particles/ml of suspension. It can be seen that the raw particle counts by BAMS significantly undercounted particles less than 1 μm in diameter. However, when equation 1 was applied to account for known BAMS sampling biases, this was partially corrected for in the final calculation of particle concentration over most of the detected particle size range. Table 2 lists the total particle concentrations in the bioaerosol chamber, regardless of identity, measured by the APS and BAMS over the first 60 s of the aerosolization of the three different concentrations of *M. smegmatis* suspensions. These values included all of the particles (>0.523 μm) generated during the experiments, with corrections for sampling biases in both systems. The particle concentrations measured by both APS and BAMS agreed fairly well, except for the range of particles with diameters of <0.7 μm. BAMS was relatively insensitive to particles in this smaller particle size range due to their low transmission efficiencies, as depicted in Fig. 2A and B. The results presented in Table 2 and the size distributions shown in Fig. 5A and B show that as a particle counter and sizer, overall BAMS remained fairly consistent with the APS.

Table 3 lists the *M. smegmatis* CFU/liter of air measured by the Andersen six-stage sampler and the BAMS measured concentration of particles classified as vegetative-cell-containing particles/liter of air in the bioaerosol chamber samples generated in the first 60 s of aerosolization of the same three concentrations of *M. smegmatis* suspensions presented in Table 2. Table 4 lists the *M. tuberculosis* H37Ra CFU/liter of air measured by the Andersen six-stage sampler and the BAMS measured concentration of particles classified as *M. tuberculosis* H37Ra-containing particles/liter of air in the bioaerosol chamber samples generated in the first 60 s of aerosolization of three different concentrations of *M. tuberculosis* H37Ra sus-

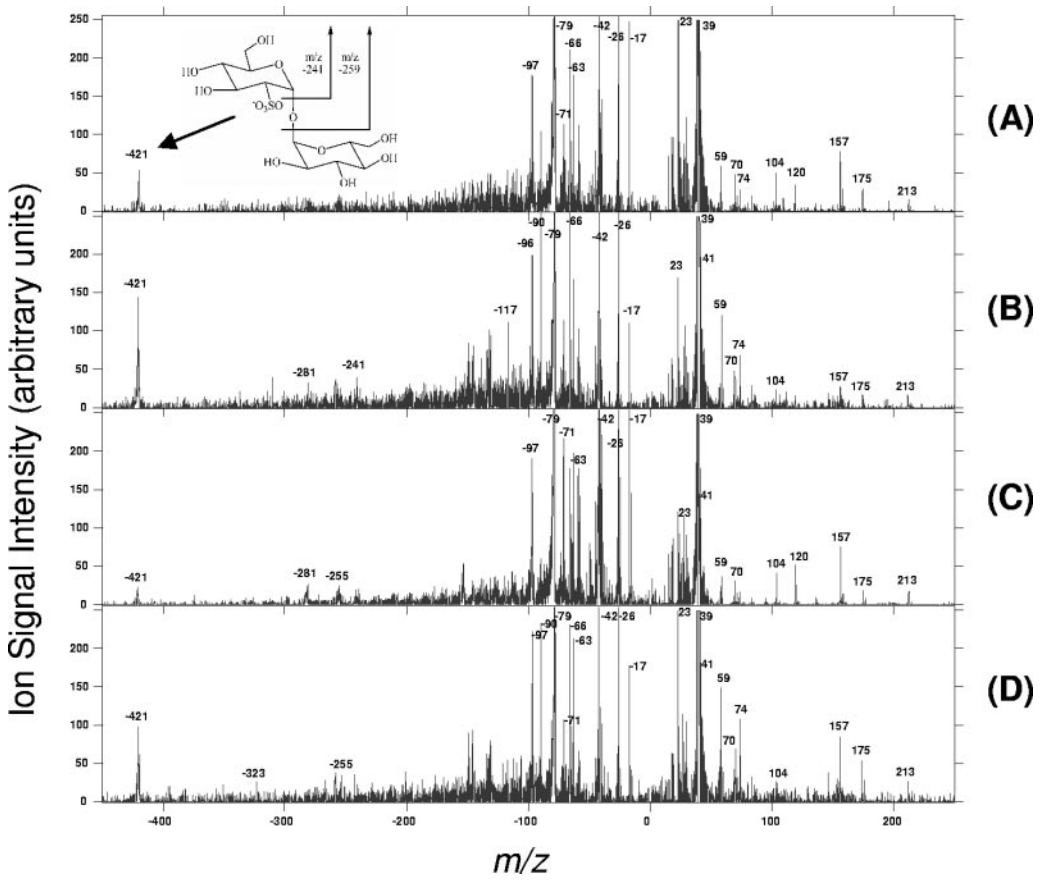

FIG. 4. Series of single-particle mass spectra from *M. tuberculosis* H37Ra-containing particles randomly selected to depict the typical wide variation in the m/z −421 signal intensity. It should also be noted that a subset of single-particle mass spectra from *M. tuberculosis* H37Ra-containing particles (~34%) contain no significant signal at m/z −421. Within panel A is the structure of deprotonated trehalose-2-sulfate, the tentative identification of the m/z −421 peak.

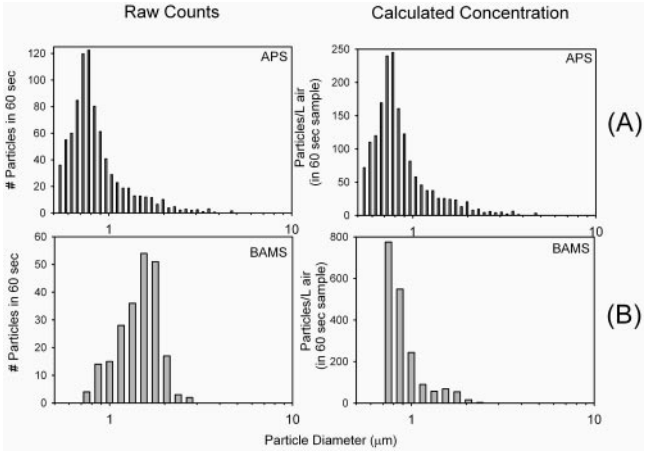

FIG. 5. Raw particle counts and calculated particle concentrations, regardless of their identity, as a function of particle diameter during the aerosolization of the high-concentration suspension (10^8 *M. smegmatis* particles/ml) into the bioaerosol chamber measured by the APS (A) and BAMS (B) in the first 60 s of aerosolization.

pensions. For the *M. tuberculosis* H37Ra samples, the cell concentrations measured by BAMS were up to two to three times higher than the CFU concentrations as measured by the viable Andersen six-stage sampler, whereas, for the *M. smegmatis* samples, the cell concentrations measured by BAMS was approximately 10 to 100 times higher than the CFU concentrations measured by the viable Andersen six-stage sampler. Here, BAMS measurements were consistently higher than the Andersen six-stage sampler measurements. This is most probably due to the fact that BAMS measures both culturable and nonculturable cells, whereas the Andersen six-stage sampler

TABLE 2. Total particle concentrations measured in the bioaerosol chamber during the first 60 s of aerosolization of *M. smegmatis* suspensions

Collison nebulizer (no. of *M. smegmatis* particles/ml)	Total no. of particles/liter of air[a] ± SD	
	APS	BAMS
1.0×10^7	53.4 ± 10.3	50.6 ± 39.4
5.0×10^7	533.0 ± 32.6	423.8 ± 85.4
1.0×10^8	1,676.4 ± 57.9	1,858.8 ± 420.0

[a] All values include only particles with diameters of >0.523 μm and are corrected for sampling biases. Equation 1 was used to calculate concentrations measured by BAMS.

TABLE 3. Concentrations of vegetative-cell-containing particles measured in the bioaerosol chamber during the first 60 s of aerosolization of *M. smegmatis* suspensions[a]

Collison nebulizer (no. of *M. smegmatis* particles/ml)	Andersen six-stage (no. of *M. smegmatis* CFU/liter of air ± SD)	BAMS (no. of vegetative-cell containing particles/ liter of air ± SD)
1.0×10^7	3.5 ± 0.4	267.3 ± 224.3
5.0×10^7	35.0 ± 1.1	506.0 ± 259.1
1.0×10^8	92.0 ± 1.8	913.8 ± 300.4

[a] All values include only particles with diameters of >0.523 μm and are corrected for sampling biases. Equation 2 was used to calculate concentrations measured by BAMS.

TABLE 5. Concentrations of vegetative-cell-containing particles measured in the bioaerosol chamber during the full 20 min of aerosolization of *M. smegmatis* suspensions[a]

Collison nebulizer (no. of *M. tuberculosis* H37Ra particles/ml)	Direct count of filter cassette sampler-collected cells (no. of cells/liter of air ± SD)	BAMS (no. of vegetative-cell containing particles/liter of air ± SD)
1.0×10^7	10.0 ± 0.4	14.4 ± 11.2
5.0×10^7	47.3 ± 0.8	42.4 ± 17.4
1.0×10^8	33.8 ± 0.7	136.9 ± 23.2

[a] All values include only particles with diameters of >0.523 μm and are corrected for sampling biases. Equation 2 was used to calculate concentrations measured by BAMS.

measures only culturable cells. Therefore, the measurement of higher concentrations of cells by BAMS relative to the viable Andersen six-stage sampler would be expected if a subset of the aerosolized cells were nonculturable. In addition, the discrepancy between the BAMS measurements and the Andersen six-stage sampler was much greater for *M. smegmatis* cells. The reason for this is unknown; however, one possibility may be that there is a significant variation in the culturability of the two organisms under the conditions in the present study. This difference in culturability could be due to the relative susceptibility of each organism to stresses such as prior preparative conditions, the washing of the cells, the aerosolization process, and impaction onto the agar plates (22, 42, 47). At this time, it is not known whether such a difference in culturability exists for *M. smegmatis* and *M. tuberculosis* H37Ra under the conditions in the present study. Further work will be required to address this issue.

The results of the BAMS measurements and the direct counts of filter cassette sampled cells over 20 min of aerosolization of the same experiments as described above for *M. smegmatis* and *M. tuberculosis H37Ra* are listed in Tables 5 and 6, respectively. Overall, particle concentrations over 20 min of aerosolization were lower than that for the first 60 s in these experiments. This may have been due to clumping of mycobacteria in the recirculated nebulizer cell suspension over time and/or continued decrease in cell concentrations in the nebulizer cell suspension over time during the 20-min aerosolization process. Nevertheless, the direct counts of filter cassette-sampled cells measure both culturable and nonculturable cells and therefore should be comparable to BAMS measurements. The BAMS measurements were relatively consistent with the direct counts of filter cassette sampled *M. smegmatis* particles but were consistently higher than the direct counts of filter cassette sampled *M. tuberculosis* H37Ra particles. In addition, the direct counts of filter cassette-sampled *M. smegmatis* particles were 10 to 30 times greater than for *M. tuberculosis* H37Ra particles when similar nebulizer cell suspension concentrations used in the experiments are compared. This suggests an even greater discrepancy between the number of measured cells and CFU for the two organisms. The reason for this observation is unknown but may be due to a combination of sources. One potential source is the issue of variations in cell culturability as discussed above. A second possible source may be an artifact of the staining process used for the direct counts of filter cassette sampled cells, where there may be a different rate of stain penetration through the cell walls of the two different organisms. A third potential source may be a variable rate of clumping of the two organisms in the nebulizer cell suspension during the aerosolization process over time. Mycobacteria, especially *M. tuberculosis* H37Ra, are known to clump easily in the absence of agents, such as Tween 80, which are traditionally used to prevent excessive cell clumping in suspensions over time (35). For the experiments presented here, no such anticlumping agent was used in order to generate clean particles. There was evidence that a certain degree of clumping occurred for both organisms during the aerosolization process. Figure 6A and B show the size distribution of the raw number of particles measured and the resulting calculated concentrations of each particle size measured for *M. tuberculosis* H37Ra-containing particles by BAMS and the Andersen six-stage sampler, respectively, in the bioaerosol chamber sample generated in the first 60 s of aerosolization of the $\sim 2 \times 10^8$ *M. tuberculosis* H37Ra particles/ml of suspension. The Andersen six-stage sampler measured an abundance of CFU measured at the

TABLE 4. Concentrations of *M. tuberculosis* H37Ra-containing particles measured in the bioaerosol chamber during the first 60 s of aerosolization of *M. tuberculosis* H37Ra suspensions[a]

Collison nebulizer (no. of *M. tuberculosis* H37Ra particles/ml)	Andersen six-stage samples (no. of *M. tubercolosis* H37Ra CFU/liter of air ± SD)	BAMS (no. of *M. tubercolosis* H37Ra particles/liter of air ± SD)
1.0×10^7	32.6 ± 1.1	62.2 ± 62.2
5.0×10^7	94.0 ± 1.8	264.3 ± 189.0
2.0×10^8	265.0 ± 3.1	333.9 ± 190.3

[a] All values include only particles with diameters of >0.523 μm and are corrected for sampling biases. Equation 2 was used to calculate concentrations measured by BAMS.

TABLE 6. Concentrations of *M. tuberculosis* H37Ra-containing particles measured in the bioaerosol chamber during the full 20 min of aerosolization of *M. tuberculosis* H37Ra suspensions[a]

Collison nebulizer no. of (*M. tuberculosis* H37Ra particles/ml)	Direct count of filter cassette sampler-collected cells (no. of cells/liter of air ± SD)	BAMS (no. of *M. tuberculosis* H37Ra particles/liter of air ± SD)
1.0×10^7	0.9 ± 0.1	6.5 ± 3.9
5.0×10^7	1.4 ± 0.1	18.6 ± 9.8
2.0×10^8	13.2 ± 0.4	45.0 ± 9.1

[a] All values include only particles with diameters of >0.523 μm and are corrected for sampling biases. Equation 2 was used to calculate concentrations measured by BAMS.

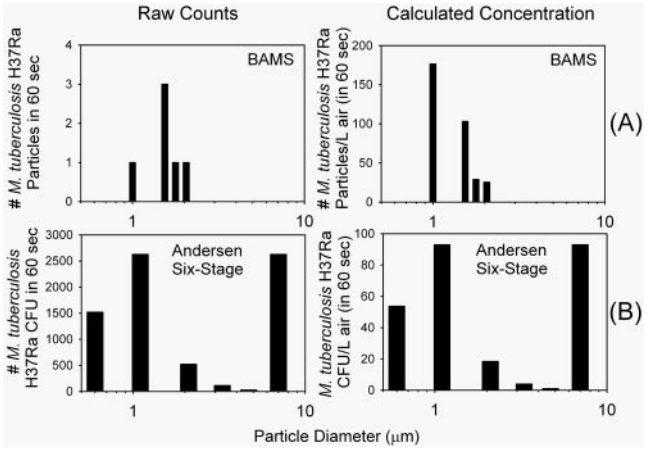

FIG. 6. Raw *M. tuberculosis* H37Ra CFU and particle counts and calculated *M. tuberculosis* H37Ra CFU and particle concentrations as a function of particle diameter during the aerosolization of the high-concentration suspension (2×10^8 *M. tuberculosis* H37Ra particles/ml) into the bioaerosol chamber as measured by BAMS (A) and the Andersen six-stage sampler (B) in the first 60 s of aerosolization.

7.0-μm cutoff. Contribution of cells to this stage of the sampler may be attributed to clumping. BAMS did not measure any *M. tuberculosis* H37Ra particles in the size range greater than 3 μm or less than 1 μm in diameter. BAMS was relatively insensitive to particles in these larger and smaller particle size ranges due to their low transmission efficiencies, as depicted in Fig. 2B.

Statistical errors of BAMS measurements. It should be noted that the errors on some of the BAMS measurements made in the present study were estimated to be high. These errors were calculated based on counting statistics for individual particle size bins and are propagated to include all of the particle sizes. Some fairly low mycobacterium concentrations were measured in the biochamber, where, in one case, for example, only one particle was identified as containing *M. tuberculosis* H37Ra. Unfortunately, much higher sample concentrations were not explored in the present study due to limitations in the aerosolization process of the mycobacteria used and the inability to quantify when the filters and Andersen six-stage sampler plates are overloaded at such levels. In addition to problems with counting statistics, the particles measured were within the size range of ~0.7 to 2.0 μm in diameter, where the correction for the BAMS sampling bias is very sensitive to particle diameter and, therefore, is very susceptible to uncertainty. This is reflected in Fig. 5B. In order to improve the confidence of the BAMS measurements at these lower agent concentrations, particle counts within the system need to be increased and sampling biases across the size range of interest (0.8 to 10 μm) need to be reduced. A novel sampling inlet with better particle transmission and focusing over a wide particle size range is currently under development in order to address this problem.

Conclusions. We presented here an initial step in the development of BAMS toward a rapid, stand-alone, airborne *M. tuberculosis* particle detector. This is the first time a potentially unique biomarker was measured in *M. tuberculosis* H37Ra at the single-cell and single-particle level in real time. A biological particle detector that could detect and identify various airborne bacterial spores (8, 34, 41), vegetative cells, viruses, and biological toxins is the overall goal of these studies. Below, we present some of the improvements we are currently developing in order for BAMS to mature towards a detector that is useful in more realistic environmental backgrounds expected in a multitude of diagnostic scenarios, such as dirty air and respiratory effluent. The first step, which we demonstrated here, is the feasibility of BAMS for the selective detection and discrimination of relatively pure *M. tuberculosis* H37Ra from *M. smegmatis* in a fairly clean aerosol background using a potentially unique metabolic marker. From the quantitative results in the present study, it can be estimated that BAMS can detect *M. tuberculosis* H37Ra containing particles at concentrations >40 *M. tuberculosis* H37Ra CFU/liter of air in 1 min in a background-free environment and compares well with the standard of cell culture. However, the overall detection limit of these clean particles alone may be improved by increasing the particle sampling efficiency through the development of an enhanced particle inlet. Furthermore, low intracellular concentrations of potential biomarkers and/or agent mixed, clumped, or coated with some background material, such as dust or sputum, can also interfere with efficient detection. As a result, we are currently developing more targeted laser desorption/ionization schemes and a higher sensitivity, higher-mass-range TOF-MS in order to improve the robustness of unique biomarkers.

ACKNOWLEDGMENTS

We thank Todd Brethauer and Paul Baron for helpful discussions. We also thank Elaine Mathews for preparation of the agar plates and media, Keith Coffee for BAMS support, and Paul Steele for data analysis software support. We also thank both the Lawrence Livermore National Laboratory and the Technical Support Working Group for their support.

This study was performed under the auspices of the U.S. Department of Energy by the University of California, Lawrence Livermore National Laboratory, under contract W-7405-Eng-48. Funding was provided by the Lawrence Livermore National Laboratory through Laboratory Directed Research and Development grant ERD-002 and the Technical Support Working Group within the Department of Defense.

REFERENCES

1. **Anderson, A. A.** 1958. New sampler for the collection, sizing, and enumeration of viable airborne particles. J. Bacteriol. **76:**471–484.
2. **Barry, C. E., R. E. Lee, K. Mdluli, A. E. Sampson, B. G. Schroeder, R. A. Slayden, and Y. Yuan.** 1998. Mycolic acids: structure, biosynthesis, and physiological functions. Prog. Lipid Res. **37:**143–179.
3. **Bright, J. J., M. A. Claydon, M. Soufian, and D. B. Gordon.** 2002. Rapid typing of bacteria using matrix-assisted laser desorption ionization time-of-flight mass spectrometry and pattern recognition software. J. Microbiol. Methods **48:**127–138.
4. **Butler, W. R., and L. S. Guthertz.** 2001. Mycolic acid analysis by high performance liquid chromatography for identification of *Mycobacterium* species. Clin. Microbiol. Rev. **14:**704–726.
5. **Corbett, E. L., C. J. Watt, N. Walker, D. Maher, B. G. Williams, M. Raviglione, and C. Dye.** 2003. The growing burden of tuberculosis: global trends and interactions with the HIV epidemic. Arch. Intern. Med. **163:**1009–1021.
6. **Fennelly, K. P., J. W. Martyny, K. E. Fulton, I. M. Orme, D. M. Cave, and L. B. Heifets.** 2004. Cough-generated aerosols of *Mycobacterium tuberculosis*: a new method to study infectiousness. Am. J. Respir. Crit. Care Med. **169:**604–609.
7. **Fenselau, C., and P. A. Demirev.** 2001. Characterization of intact microorganisms by MALDI mass spectrometry. Mass Spectrom. Rev. **20:**157–171.
8. **Fergenson, D. P., M. E. Pitesky, H. J. Tobias, P. T. Steele, G. A. Czerwieniec, S. C. Russell, C. Lebrilla, J. Horn, K. Coffee, A. Srivastava, S. P. Pillai, M.-T. P. Shih, H. L. Hall, A. J. Ramponi, J. T. Chang, R. G. Langlois, P. L. Estacio, R. T. Hadley, M. Frank, and E. Gard.** 2004. Reagentless detection

and classification of individual bioaerosol particles in seconds. Anal. Chem. **76:**373–378.

9. **Fox, A., R. M. T. Rosario, and L. Larsson.** 1993. Monitoring of bacterial sugars and hydroxy fatty acids in dust from air conditioners by gas chromatography-mass spectrometry. Appl. Environ. Microbiol. **59:**4354–4360.
10. **Frieden, T. R., T. R. Sterling, S. S. Munsiff, C. J. Watt, and C. Dye.** 2003. Tuberculosis. Lancet **362:**887–899.
11. **Gard, E., J. E. Mayer, B. D. Morrical, T. Dienes, D. P. Fergenson, and K. A. Prather.** 1997. Real-time analysis of individual atmospheric aerosol particles: design and performance of a portable ATOFMS. Anal. Chem. **69:**4083–4091.
12. **Garg, S. K., R. P. Tiwari, D. Tiwari, R. Singh, D. Malhotra, V. K. Ramnani, G. B. K. S. Prasad, R. Chandra, M. Fraziano, V. Colizzi, and P. S. Bisen.** 2003. Diagnosis of tuberculosis: available technologies, limitations, and possibilities. J. Clin. Lab. Anal. **17:**155–163.
13. **Gieray, R. A., P. T. Reilly, M. Yang, W. B. Whitten, and J. M. Ramsey.** 1997. Real-time detection of individual airborne bacteria. J. Microbiol. Methods **29:**191–199.
14. **Griffin, P., D. McClenahan, and J. VandeVelde.** 2004. Tuberculosis transmission in multiple correctional facilities–Kansas, 2002–2003. Morb. Mortal. Wkly. Rep. **53:**734–738.
15. **Hamasur, B., J. Bruchfeld, M. Haile, A. Pawlowski, B. Bjorvatn, G. Kallenius, and S. B. Svenson.** 2001. Rapid diagnosis of tuberculosis by detection of mycobacterial lipoarabinomannan in urine. J. Microbiol. Methods **45:**41–52.
16. **Hinz, K. P., M. Greweling, F. Drews, and B. Spengler.** 1999. The data processing in on-line laser mass spectrometry of inorganic, organic, or biological airborne particles. J. Am. Soc. Mass Spectrom. **10:**648–660.
17. **Huggett, J. F., T. D. McHugh, and A. Zumla.** 2003. Tuberculosis: amplification-based clinical diagnostic techniques. Int. J. Biochem. Cell Biol. **35:**1407–1412.
18. **Johnston, M. V., and A. S. Wexler.** 1995. MS of individual aerosol particles. Anal. Chem. **67:**A721–A726.
19. **Kievit, O., M. Weiss, P. T. Verheijen, J. M. Marijnissen, and B. Scarlett.** 1996. The on-line chemical analysis of single particles using aerosol beams and time-of-flight mass spectrometry. Chem. Eng. Commun. **151:**79–100.
20. **Laval, F., M.-A. Laneelle, C. Deon, B. Monsarrat, and M. Daffe.** 2001. Accurate molecular mass determination of mycolic acids by MALDI-TOF mass spectrometry. Anal. Chem. **73:**4537–4544.
21. **Lever, M. S., A. Williams, and A. M. Bennett.** 2000. Survival of mycobacterial species in aerosols generated from artificial saliva. Lett. Appl. Microbiol. **31:**238–241.
22. **Marthi, B., V. P. Fieland, M. V. Walter, and R. J. Seidler.** 1990. Survival of bacteria during aerosolization. Appl. Environ. Microbiol. **56:**3463–3467.
23. **Marvin, L. F., M. A. Roberts, and L. B. Fay.** 2003. Matrix-assisted laser desorption/ionization time-of-flight mass spectrometry in clinical chemistry. Clin. Chim. Acta **337:**11–21.
24. **Mayakova, T. I., E. E. Kuznetsova, M. G. Kovaleva, and S. A. Plyusnin.** 1995. Gas chromatography-mass spectrometric study of lipids and rapid diagnosis of *Mycobacterium tuberculosis*. J. Chromatogr. B **672:**133–137.
25. **McKeown, P. J., M. V. Johnston, and D. M. Murphy.** 1991. On-line single-particle analysis by laser desorption mass spectrometry. Anal. Chem. **63:**2069–2073.
26. **Mougous, J. D., R. E. Green, S. J. Williams, S. E. Brenner, and C. R. Bertozzi.** 2002. Sulfotransferases and sulfatases in mycobacteria. Chem. Biochem. **9:**767–776.
27. **Mougous, J. D., M. D. Leavell, R. H. Senaratne, C. D. Leigh, S. J. Williams, L. W. Riley, J. A. Leary, and C. R. Bertozzi.** 2002. Discovery of sulfated metabolites in mycobacteria with a genetic and mass spectrometric approach. Proc. Natl. Acad. Sci. **99:**17037–17042.
28. **Mougous, J. D., C. J. Petzold, R. H. Senaratne, D. H. Lee, D. L. Akey, F. L. Lin, S. E. Munchel, M. R. Pratt, L. W. Riley, J. A. Leary, J. M. Berger, and C. R. Bertozzi.** 2004. Identification, function and structure of the mycobacterial sulfotransferase that initiates sulfolipid-1 biosynthesis. Nat. Struct. Mol. Biol. **11:**721–729.
29. **Murphy, D. M., and D. S. Thomson.** 1995. Laser ionization mass spectroscopy of single aerosol particles. Aerosol Sci. Technol. **22:**237–249.
30. **Noble, C. A., and K. A. Prather.** 2000. Real-time single particle mass spectrometry: a historical review of a quarter century of the chemical analysis of aerosols. Mass Spectrom. Rev. **19:**248–274.
31. **Parker, E. P., M. W. Trahan, J. S. Wagner, S. E. Rosenthal, W. B. Whitten, R. A. Gieray, P. T. Reilly, A. C. Lazar, and J. M. Ramsey.** 2000. Detection and classification of individual airborne microparticles using laser ablation mass spectrometry and multivariate analysis. Field Anal. Chem. Technol. **4:**31–42.
32. **Peters, T. M., and D. Leith.** 2003. Concentration measurement and counting efficiency of the aerodynamic particle sizer 3321. J. Aerosol Sci. **34:**627–634.
33. **Phares, D. J., K. P. Rhoads, A. S. Wexler, D. B. Kane, and M. V. Johnston.** 2001. Application of the ART-2a algorithm to laser ablation aerosol mass spectrometry of particle standards. Anal. Chem. **73:**2338–2344.
34. **Russell, S. C., G. Czerwieniec, H. Tobias, D. P. Fergenson, P. Steele, M. Pitesky, J. Horn, A. Srivastava, M. Frank, E. E. Gard, and C. Lebrilla.** 2004. Toward understanding the ionization of biomarkers from micrometer particles by bio-aerosol mass spectrometry. J. Am. Soc. Mass Spectrom. **15:**900–909.
35. **Schafer, M. P., J. E. Fernbach, and M. K. Ernst.** 1999. Detection and characterization of airborne *Mycobacterium tuberculosis* H37Ra particles, a surrogate for airborne pathogenic *M. tuberculosis*. Aerosol Sci. Technol. **30:**161–173.
36. **Schafer, M. P., J. E. Fernbach, and P. A. Jensen.** 1998. Sampling and analytical method development for qualitative assessment of airborne mycobacterial species of the *Mycobacterium tuberculosis* complex. Am. Ind. Hyg. Assoc. **59:**540–546.
37. **Schafer, M. P., K. F. Martinez, and E. S. Matthews.** 2003. Rapid detection and determination of the aerodynamic size range of airborne mycobacteria associated with whirlpools. Appl. Occup. Environ. Hyg. **18:**41–50.
38. **Sinha, M. P., R. M. Platz, S. K. Friedlander, and V. L. Vilker.** 1985. Characterization of bacteria by particle beam mass spectrometry. Appl. Environ. Microbiol. **49:**1366–1373.
39. **Sinha, M. P., R. M. Platz, V. L. Vilker, and S. K. Friedlander.** 1984. Analysis of individual biological particles by mass spectrometry. Int. J. Mass Spectrom. Ion Proc. **57:**125–133.
40. **Song, X.-H., P. K. Hopke, D. P. Fergenson, and K. A. Prather.** 1999. Classification of single particles analyzed by ATOFMS using an artificial neural network, ART-2a. Anal. Chem. **71:**860–865.
41. **Steele, P. T., H. J. Tobias, D. P. Fergenson, M. E. Pitesky, J. M. Horn, G. A. Czerwieniec, S. C. Russell, C. Lebrilla, E. E. Gard, and M. Frank.** 2003. Laser power dependence of mass spectral signatures from individual bacterial spores in bioaerosol mass spectrometry. Anal. Chem. **75:**5480–5487.
42. **Stewart, S. L., S. A. Grinshpun, K. Willeke, S. Terzieva, V. Ulevicius, and J. Donnelly.** 1995. Effect of impact stress on microbial recovery on an agar surface. Appl. Environ. Microbiol. **61:**1232–1239.
43. **Stowers, M. A., A. L. v. Wuijckhuijse, J. M. Marijnissen, B. Scarlett, B. M. v. Baar, and C. E. Kientz.** 2000. Application of matrix-assisted laser desorption/ionization to on-line aerosol time-of-flight mass spectrometry. Rapid Commun. Mass Spectrom. **14:**829–833.
44. **Suess, D. T., and K. A. Prather.** 1999. Mass spectrometry of aerosols. Chem. Rev. **99:**3007–3035.
45. **Tevere, V. J., P. L. Hewitt, A. Dare, P. Hocknell, A. Keen, J. P. Spadoro, and K. K. Young.** 1996. Detection of *Mycobacterium tuberculosis* by PCR amplification with Pan-*Mycobacterium* primers and hybridization to an *M. tuberculosis*-specific probe. J. Clin. Microbiol. **34:**918–923.
46. **Verma, G., R. E. G. Upshur, E. Rea, and S. R. Benatar.** 2004. Critical reflections on evidence, ethics, and effectiveness in the management of tuberculosis: public health and global perspectives. BMC Med. Ethics **5:**E2–E8.
47. **Walter, M. V., B. Marthi, V. P. Fieland, and L. M. Ganio.** 1990. Effect of aerosolization on subsequent bacterial survival. Appl. Environ. Microbiol. **56:**3468–3472.
48. **Watanabe, M., Y. Aoyagi, M. Ridell, and D. E. Minnikin.** 2001. Separation and characterization of individual mycolic acids in representative mycobacteria. Microbiology **147:**1825–1837.
49. **Woodruff, P. J., B. L. Carlson, B. Siridechadilok, M. R. Pratt, R. H. Senaratne, J. D. Mougous, L. W. Riley, S. J. Williams, and C. R. Bertozzi.** 2004. Trehalose is required for growth of *Mycobacterium smegmatis*. J. Biol. Chem. **279:**28835–28843.